Electroweak Physics in the Forward Region at the LHC

S. Farry ([1])([*])

([1]) *University of Liverpool - Liverpool, United Kingdom*

Summary. — The unique forward acceptance of LHCb covers a range of rapidities not accessible by the other LHC experiments and provides unique and complementary information to measurements performed in the central region. Recent measurements of electroweak boson production at LHCb using both the Run-I and Run-II datasets are presented.

PACS 13.38.Be – Decays of W bosons.
PACS 13.38.Dg – Decays of Z bosons.

1. – Introduction

The LHCb detector [1] is a dedicated forward detector at the LHC, fully instrumented in the pseudorapidity region $2.0 < \eta < 5.0$. Studies of the production and decay of electroweak bosons in the forward region provide both complementary and unique information to measurements performed in the central region. As forward bosons are produced through the annihilation of two partons with asymmetric longitudinal proton momentum fractions, studies of their production simultaneously probe the low- and high-x regions of the (x, Q^2) plane, providing constraints on the parton distribution functions (PDFs) in a unique region of phase space. In addition, the forward-backward asymmetry of Z decays is more prominent in the forward region at a proton-proton collider such as the LHC. As Z bosons produced at forward rapidities are more likely to follow the initial quark direction, they suffer less from the dilution of the parton level asymmetry observed in the central region. This makes LHCb particularly sensitive to a measurement of the weak mixing angle, $\sin^2\theta_W^{\rm eff}$.

As the LHCb detector has been optimised to identify and reconstruct b and c hadron decays through precision tracking, vertexing, and particle identification, it is also ideally suited to the reconstruction and identification of heavy flavour jets, which can be exploited in order to make measurements of electroweak boson production in association with b- and c- jets.

([*]) On Behalf of the LHCb Collaboration.

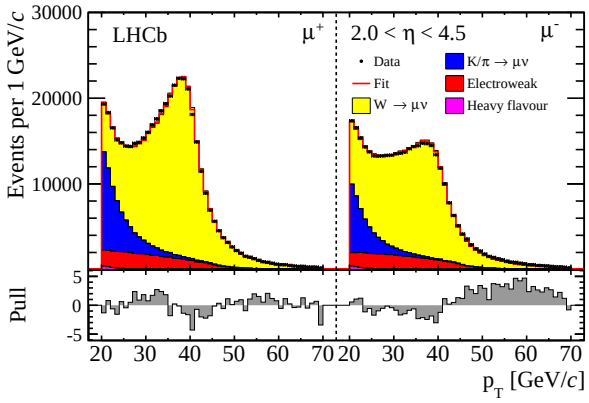

Fig. 1. – Fit to the p_{T} spectrum of muon candidates in the 7 TeV data sample for W^+ (left) and W^- (right) candidates for purity extraction.

2. – Inclusive W boson production

The LHCb experiment has measured inclusive W boson production in the forward region using data collected during Run-I of the LHC at centre-of-mass energies of 7 and 8 TeV [2, 3], corresponding to integrated luminosities of 1 and 2 fb^{-1} respectively. Events are selected which contain muons with a transverse momentum of greater than 20 GeV and a pseudorapidity in the region $2.0 < \eta < 4.5$. The muons are required to be isolated and to have a small impact parameter with respect to any primary vertex. The purity of the selected W boson sample is determined by performing a template fit to the p_{T} of the selected muon candidates using signal and background shapes obtained from a mixture of data and simulation. The signal shape and the dominant background, arising from muons produced through the decay-in-flight of pions and kaons, are allowed to float in the fit, with the other backgrounds normalised using data-driven techniques. The fit is shown for both positively and negatively charged muons candidates selected in the 7 TeV dataset in fig. 1 with a purity of approximately 77% achieved. The extracted yields are corrected for detector reconstruction and selection efficiency, as well as final state radiation in order to facilitate a comparison with Born level QCD predictions. The differential cross-section and lepton charge asymmetry at 7 and 8 TeV respectively are shown in fig. 2 as a function of lepton pseudorapidity. The results are compared to predictions obtained at NNLO in perturbative QCD using the FEWZ generator [4] and a number of different PDF sets with a good level of agreement observed. The experimental precision is dominated by the luminosity measurement, as well as the effect of the beam energy uncertainty, with both sources contributing uncertainties of 1-2%.

3. – Inclusive Z boson production

Measurements have also been performed at LHCb of inclusive Z boson production in the muon [2, 3] and electron [5, 6] decay channels at 7 and 8 TeV. The same kinematic selection is applied as in the case of W production, where a second, opposite-sign lepton is also required to be present and the pair are required to form an invariant mass in the

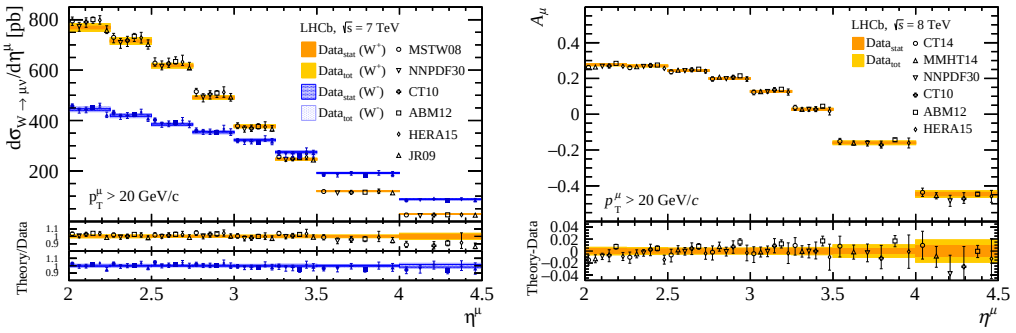

Fig. 2. – Measurements of (left) the W boson production cross-section at 7 TeV and (right) the lepton charge asymmetry at 8 TeV, where both are shown as a function of lepton pseudorapidity and compared to NNLO QCD predictions using a variety of PDF sets [2, 3].

region of the Z peak. In the dimuon channel, this is chosen to be between 60 and 120 GeV, while for the electron channel, incomplete Bremsstrahlung recovery results in the smearing of the mass spectrum to lower masses, and so the di-electron invariant mass is required to be larger than 40 GeV, and the measurement is corrected to the same fiducial as the $Z \to \mu\mu$ channel using simulation. The purity is determined using data-driven methods to be over 99% for the dimuon channel, and approximately 95% in the electron channel. The measurements are corrected for detector and selection efficiency, as well as final state radiation and presented as a function of boson rapidity in fig. 3, with a similar level of agreement observed as in the case of W boson production. Uncertainties on the overall normalisation due to the luminosity and the beam energy are again seen to dominate, where it should be noted that the beam energy uncertainty is only applied to the $Z \to \mu\mu$ measurements.

A preliminary measurement of Z boson production at 13 TeV using the Run-II dataset

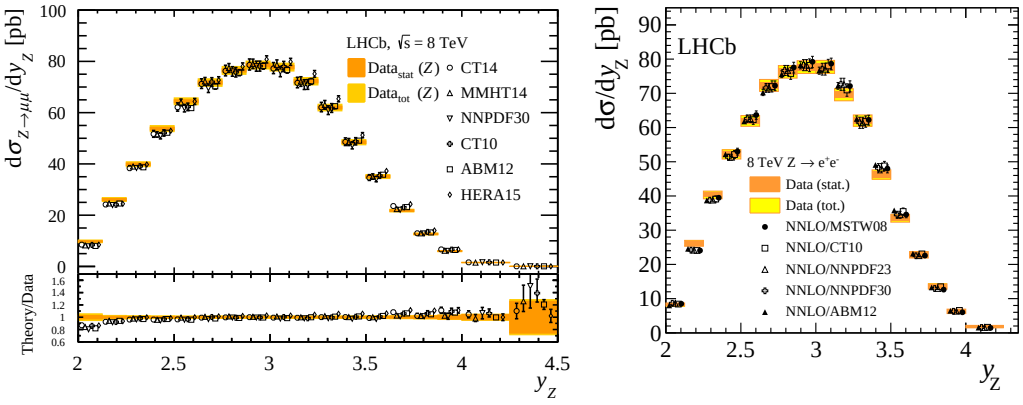

Fig. 3. – Measurements of the Z boson production cross-section measured at LHCb at 8 TeV for the (left) muon and (right) electron decay mode. Comparisons are made to NNLO QCD predictions with a range of PDF sets [2, 6].

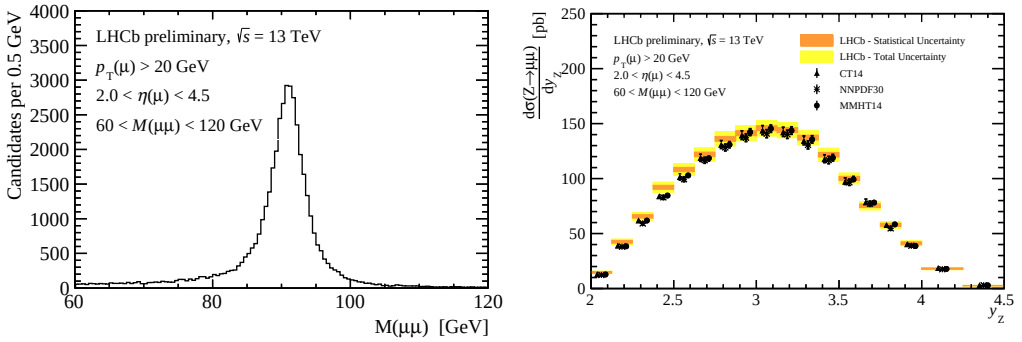

Fig. 4. – The $Z \to \mu\mu$ (left) mass spectrum and (right) differential production cross-section as a function of rapidity measured at a centre-of-mass energy of 13 TeV. Comparisons are made to NNLO QCD predictions using three different PDF sets [7].

has also been performed using a dataset corresponding to approximately 300 pb^{-1} [7]. The same selection is applied as for the Run-I measurements, and the dominant uncertainty of 3.9% arises from the knowledge of the integrated luminosity of the 2015 dataset. The $Z \to \mu\mu$ mass spectrum and differential production cross-section as a function of rapidity are shown in fig. 4.

4. – Forward-backward asymmetry and extraction of $\sin^2\theta_W^{\text{eff}}$

The annihilation process $q\bar{q} \to \ell^+\ell^-$ exhibits a forward-backward asymmetry, A_{FB}, due to the presence of both vector and axial-vector amplitudes. The asymmetry is observed when considering the distribution of the polar angle of the negative lepton, measured with respect to the quark direction in the $q\bar{q}$ rest frame. It shows a strong dependence on the dilepton invariant mass near the Z resonance. As the LHC is a symmetric pp collider, the quark direction is not known and the forward direction is alternatively defined with respect to the z component of the Z boson momentum. This results in a dilution of the asymmetry in cases where the Z boson does not follow the direction of the initial quark. As the valence quarks are more prominent in the forward region, a consequence of the higher x-region probed, the parton level asymmetry is more pronounced in this region.

The measurement of Z boson production outlined in sect. **3** is extended to perform a measurement of A_{FB} as a function of dilepton invariant mass in the dimuon channel at LHCb [8]. The measurement has been performed using data collected at both 7 and 8 TeV in Run-I. The distributions obtained from data are corrected for background contributions and unfolded for detector effects to obtain the true asymmetry distributions, shown in fig. 5. The dominant uncertainty on the measurements arise from the knowledge of the muon momentum.

As A_{FB} is sensitive to the effective weak mixing angle, the measurement has been extended in order to extract the value of $\sin^2\theta_W^{\text{eff}}$ using a template fit to the measured asymmetry. Templates are obtained using theoretical predictions with a range of values of $\sin^2\theta_W^{\text{eff}}$ and a χ^2 minimisation is performed in order to determine the best fit value. The templates are generated using POWHEGBOX [9] interfaced with PYTHIA8 where the NNPDF2.3 PDF set is used to describe the colliding protons. The extracted value is

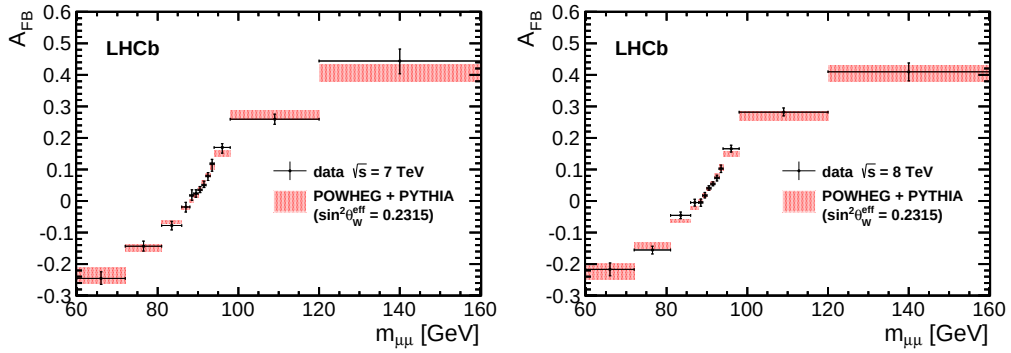

Fig. 5. – The measured forward backward asymmetries at (left) 7 and (right) 8 TeV compared to predictions obtained from the PowhegBox generator using the NNPDF2.3 PDF set and interfaced with Pythia8. [8]

shown in fig. 6 and compared to measurements at different experiments. The LHCb measurement is statistically limited and represents the most precise measurement at the LHC, with the dominant source of systematic uncertainty due to description of the PDFs.

5. – W boson production in association with heavy flavour jets

Heavy flavour tagging at LHCb is achieved using a secondary vertex tagging algorithm, which identifies heavy flavour jets by the presence of a secondary vertex with a

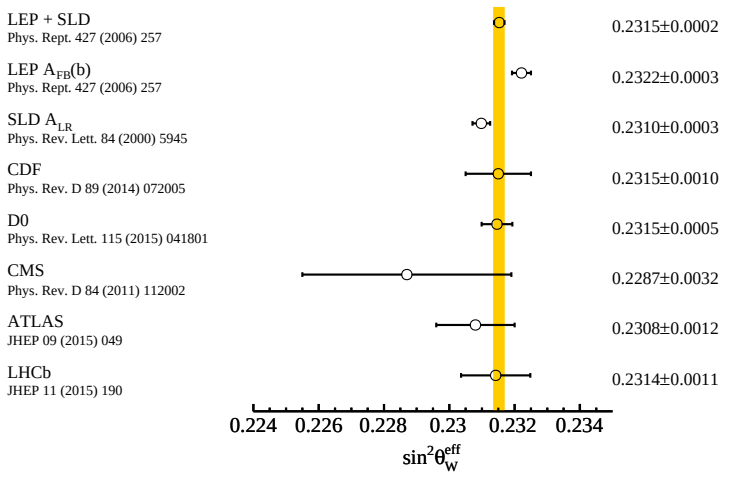

Fig. 6. – Comparison of measurements of $\sin^2\theta_W$ as performed by ATLAS, LHCb and a number of different experiments. The band shown is the combination of the results from LEP and SLD.

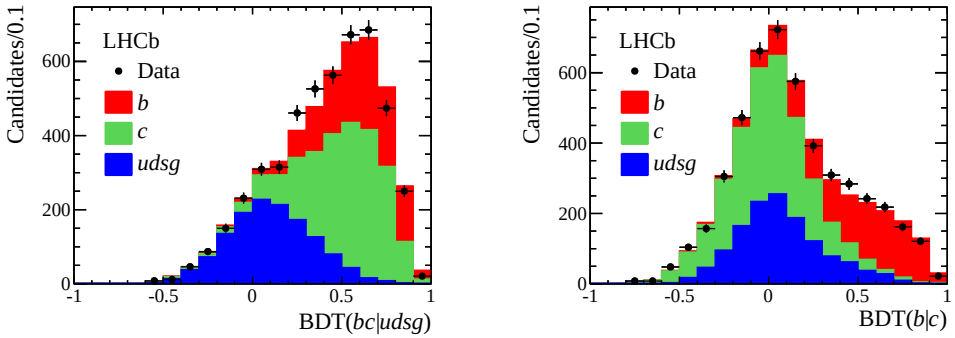

Fig. 7. – Shown are the BDT distributions used to separate (left) light jets from heavy flavour jets and (right) b-jets from c-jets in order to measure W production in association with $b-$ or $c-$ jets [10].

radial separation, $\Delta R < 0.5$ between its direction of flight and that of the jet axis. Two boosted decision trees (BDTs) are trained using characteristics of both the jet and the secondary vertex to separate light jets from heavy flavour jets, and $b-$jets from $c-$jets. More details on the secondary vertex tagging algorithm can be found in Ref. [10].

These heavy flavour tagging capabilities are exploited to perform measurements of W boson production in association with b- and c-jets. The W boson is reconstructed using a similar selection to that described in sect. **2**, and additionally a jet is required to be present with a p_{T} in excess of 20 GeV and a pseudorapidity between 2.2 and 4.2. The events are also required to satisfy $p_{\mathrm{T}}(j_\mu + j) > 20$ GeV, where j_μ is the reconstructed jet containing the muon candidate. This observable is expected to be large for W+jet events due to the missing neutrino in the final state and the requirement improves the signal purity by rejecting backgrounds arising from di-jet production where the jets are typically balanced in transverse momentum.

The presence of a high-p_{T} jet produced in association with the W boson results in a dilution of the distinctive Jacobian peak in the muon p_{T} spectrum used for purity determination in the inclusive W analysis and so the purity is instead extracted using a fit to an isolation variable. This variable is defined as the ratio of the muon p_{T} to the p_{T} of the j_μ object. The background in the sample arising from QCD backgrounds, such as mis-id, or the semi-leptonic decay of heavy flavour mesons is then determined using fits to this variable. The b and c-jet yields are extracted by performing a fit to the two-dimensional BDT distributions in each isolation bin. Additional backgrounds are considered from other electroweak processes, such as $Z \to \mu\mu$, $Z \to \tau\tau$, $W \to \tau\nu_\tau$ and top production, and are subtracted using data-driven techniques. Fits to the BDT distributions in the $p_{\mathrm{T}}(\mu)/p_{\mathrm{T}}(j_\mu) > 0.9$ bin are shown in fig. 7.

The extracted signal yields are then corrected for detector efficiency and other reconstruction effects and measurements of production cross-sections and ratios are performed at both 7 and 8 TeV. The ratios of Wb and Wc production to inclusive Wj production, and their charge asymmetries are shown in fig. 8 and compared to the SM predictions obtained at NLO using MCFM [12] and the CT10 PDF set. A good agreement is in general observed.

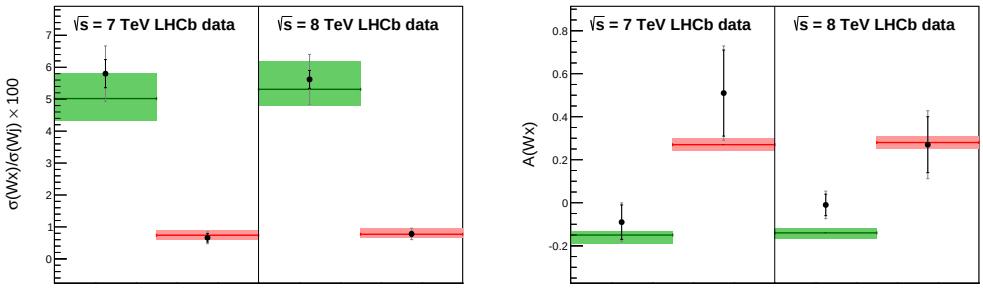

Fig. 8. – Comparisons of measurements performed at 7 and 8 TeV for Wc (green) and Wb (red) compared to theoretical predictions for (left) the ratio of Wb/Wc to Wj production and (right) Wb/Wc charge asymmetries [11].

6. – Conclusions

Measurements performed by the LHCb experiment of electroweak boson production during Run-I of the LHC have been presented. These include measurements of the inclusive production of W and Z bosons, an extraction of $\sin^2\theta_W^{\rm eff}$ through a precise measurement of the forward backward asymmetry in $Z \to \mu\mu$ decays, and measurements of the production of W bosons in association with heavy flavour jets. In addition, the first measurement of electroweak boson production in Run-II, a preliminary measurement of Z boson production at 13 TeV, has been presented. All results are seen to be in agreement with Standard Model predictions.

REFERENCES

[1] LHCb, A. A. Alves, Jr. *et al.*, *The LHCb Detector at the LHC*, JINST **3** (2008) S08005.
[2] LHCb, R. Aaij *et al.*, *Measurement of the forward Z boson production cross-section in pp collisions at* $\sqrt{s} = 7$ *TeV*, JHEP **08** (2015) 039, arXiv:1505.07024.
[3] LHCb, R. Aaij *et al.*, *Measurement of forward W and Z boson production in pp collisions at* $\sqrt{s} = 8$ *TeV*, JHEP **01** (2016) 155, arXiv:1511.08039.
[4] R. Gavin, Y. Li, F. Petriello, and S. Quackenbush, *FEWZ 2.0: A code for hadronic Z production at next-to-next-to-leading order*, Comput. Phys. Commun. **182** (2011) 2388, arXiv:1011.3540.
[5] LHCb, R. Aaij *et al.*, *Measurement of the cross-section for* $Z \to e^+e^-$ *production in pp collisions at* $\sqrt{s} = 7$ *TeV*, JHEP **02** (2013) 106, arXiv:1212.4620.
[6] LHCb, R. Aaij *et al.*, *Measurement of forward* $\mathrm{Z} \to \mathrm{e}^+\mathrm{e}^-$ *production at* $\sqrt{s} = 8$ *TeV*, JHEP **05** (2015) 109, arXiv:1503.00963.
[7] LHCb Collaboration, *Measurement of the* $Z \to \mu^+\mu^-$ *production cross-section at forward rapidities in pp collisions at* $\sqrt{s} = 13$ *TeV*, Tech. Rep. LHCb-CONF-2016-002. CERN-LHCb-CONF-2016-002, CERN, Geneva, Mar, 2016.
[8] LHCb, R. Aaij *et al.*, *Measurement of the forward-backward asymmetry in* $Z/\gamma^* \to \mu^+\mu^-$ *decays and determination of the effective weak mixing angle*, JHEP **11** (2015) 190, arXiv:1509.07645.
[9] S. Alioli, P. Nason, C. Oleari, and E. Re, *NLO vector-boson production matched with shower in POWHEG*, JHEP **07** (2008) 060, arXiv:0805.4802.

[10] LHCb, R. Aaij *et al.*, *Identification of beauty and charm quark jets at LHCb*, JINST **10** (2015), no. 06 P06013, arXiv:1504.07670.
[11] LHCb, R. Aaij *et al.*, *Study of W boson production in association with beauty and charm*, arXiv:1505.04051.
[12] J. M. Campbell and R. K. Ellis, *Radiative corrections to Z b anti-b production*, Phys. Rev. **D62** (2000) 114012, arXiv:hep-ph/0006304.